A united event grand canonical Monte Carlo study of partially doped polyaniline

M. S. Byshkin, A. Correa, F. Buonocore, A. Di Matteo, and G. Milano

Citation: The Journal of Chemical Physics **139**, 244906 (2013); doi: 10.1063/1.4848697
View online: http://dx.doi.org/10.1063/1.4848697
View Table of Contents: http://scitation.aip.org/content/aip/journal/jcp/139/24?ver=pdfcov
Published by the AIP Publishing

A united event grand canonical Monte Carlo study of partially doped polyaniline

M. S. Byshkin,[1,a)] A. Correa,[1] F. Buonocore,[2] A. Di Matteo,[3,4] and G. Milano[1,4,a)]
[1]*Modeling Lab for Nanostructure and Catalysis, Dipartimento di Chimica e Biologia and NANOMATES, University of Salerno, 84084, via Ponte don Melillo, Fisciano Salerno, Italy*
[2]*ENEA Casaccia Research Center, Via Anguillarese 301, 00123 Rome, Italy*
[3]*STMicroelectronics, Via Remo de Feo, 1 80022 Arzano, Naples, Italy*
[4]*IMAST Scarl Piazza Bovio 22, 80133 Naples, Italy*

(Received 12 August 2013; accepted 2 December 2013; published online 26 December 2013)

A Grand Canonical Monte Carlo scheme, based on united events combining protonation/deprotonation and insertion/deletion of HCl molecules is proposed for the generation of polyaniline structures at intermediate doping levels between 0% (PANI EB) and 100% (PANI ES). A procedure based on this scheme and subsequent structure relaxations using molecular dynamics is described and validated. Using the proposed scheme and the corresponding procedure, atomistic models of amorphous PANI-HCl structures were generated and studied at different doping levels. Density, structure factors, and solubility parameters were calculated. Their values agree well with available experimental data. The interactions of HCl with PANI have been studied and distribution of their energies has been analyzed. The procedure has also been extended to the generation of PANI models including adsorbed water and the effect of inclusion of water molecules on PANI properties has also been modeled and discussed. The protocol described here is general and the proposed United Event Grand Canonical Monte Carlo scheme can be easily extended to similar polymeric materials used in gas sensing and to other systems involving adsorption and chemical reactions steps. © *2013 AIP Publishing LLC*. [http://dx.doi.org/10.1063/1.4848697]

I. INTRODUCTION

Conjugated organic polymers are either electrical insulators or semiconductors. During the doping process an organic polymer, having a small conductivity is converted into a polymer which is in the "metallic" conducting regime. Both doping and reverse undoping processes may be involved chemically or electrochemically. By controllably adjusting the doping level, conjugated polymers with conductivity anywhere between that of the non-doped and that of the fully doped may be obtained.[1]

Polyaniline (PANI) is one of the most widely used conducting polymer because of its easy synthesis, high chemical and environmental stability, and tunable properties.[1,2] The emeraldine base (EB) form of PANI is especially attractive. It may be doped by adding compounds in desired quantity. The maximum doping level is reached when all imine nitrogens (half of the total nitrogens) are protonated (Fig. 1). This fully doped form is called emeraldine salt (PANI ES) and the scheme of its bipoloronic state[3,4] is presented in Fig. 1. Dopants can be removed back by interaction with a base. As doping level changes from 0% (PANI EB) to 100% (PANI ES) (Fig. 1) the conductivity varies[4,5] from 10^{-10} to 10^{0} Ω^{-1} cm^{-1}. The strong dependence of electrical conductivity on doping rate and favorable response to guest molecule makes PANI useful for gas sensors.[6,7] There are many applications in which measuring gas concentration is critical. For example, continuous monitoring of the HCl content in flue gas purification plants is a key issue for incineration facilities in order to optimize process efficiency and to ensure compliance with existing emission regulations. In the technological research area for low power sensors, conductive polymers are attractive due to their ability to operate at room temperature, to be synthesized through easy chemical or electrochemical processes, and modified conveniently by copolymerization or structural derivations.[7] Moreover, the good mechanical properties of PANI facilitate the fabrication process of sensors. On the other hand, micro- and nanopatterning of these sensing materials and formation of ultrathin sensing films facilitate enhanced vapor diffusion and response speed when compared to conventional polymeric films. There are several reviews and papers[6,7] that emphasize different aspects of gas sensors, and some others that discuss sensing performance of certain conducting polymers, but few of them pay special attention to a molecular understanding of the impact of gas molecules on the polymer matrix.

Atomistic models have already been used to study PANI. *Ab initio* and DFT simulations were extensively used to study various PANI oligomers and infinite periodic chains. In particular, besides geometric and electronic properties of oligomers, DFT and *ab initio* techniques were successfully used to study interaction of PANI oligomers with different dopants[4,8] and PANI ES optical properties.[9] Simulation with empirical potentials allowed to study amorphous PANI structures: water adsorption and diffusion in PANI ES,[10] thermal conductivity,[11] and water adsorption in PANI EB.[12] The first simulation of partially doped PANI was recently performed

a)Authors to whom correspondence should be addressed. Electronic addresses: mbyshkin@unisa.it and gmilano@unisa.it

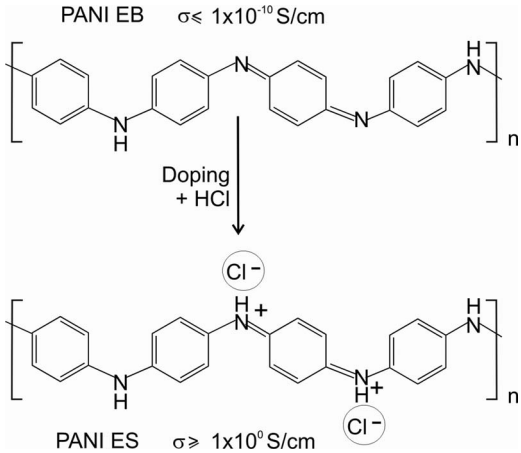

FIG. 1. PANI doping scheme.

by Chen *et al.*[13] In their model HCl molecules do not dissociate and energies of bonds between HCl and PANI are not calculated; these bonds are formed during MD simulation if the distance criteria is satisfied; by modifying the amount of HCl molecules in PANI structures and fixing the simulation time, different doping levels could be obtained.

In this paper, we propose a Grand Canonical Monte Carlo (GCMC) scheme, based on united events combining protonation/deprotonation and insertion/deletion of HCl. In particular, a procedure based on combination of MC with reactive moves aimed to generate partially doped atomistic models of amorphous PANI and MD simulations to relax these structures is proposed.

II. METHODS AND MODELS

In the present section, Subsection II A is intended to give an introduction to the proposed United Event Grand Canonical (UEGC) Monte Carlo scheme able to generate partially doped structures. Subsections II B and II C contain a description of the force-field and technical details of simulations, respectively.

A. Monte Carlo scheme for generation of partially doped PANI structures

The use of Monte Carlo or Molecular Dynamics techniques based on classical force-fields would allow to generate only amorphous structures of PANI EB or PANI ES but not of partially doped PANI, where partially doped PANI may be considered as a mixture of doped and undoped PANI units. Indeed it is evident that distribution of doped/undoped PANI units may considerably influence PANI transport properties. Therefore a UEGC Monte Carlo scheme is proposed here to generate equilibrium partially doped structures. In the present study we choose HCl as gas penetrant molecule and PANI as polymer matrix but the proposed scheme is general and different gas/polymer pairs may also be used.

The first step of the PANI doping process is the adsorption of HCl molecules into the PANI structure. For this reason MC simulation in GC ensemble may be performed, where the MC event is insertion/deletion of a HCl molecule. The probability of acceptance of this event that satisfies the detailed balance requirements[14] may be written as

$$\min[1, P_{ins}],\ P_{ins} = \frac{V}{\Lambda^3(M+1)} \exp\{-\beta((E_1 - E_0) - \mu)\}, \tag{1a}$$

when molecule is inserted, and

$$\min[1, P_{del}],\ P_{del} = \frac{\Lambda^3 M}{V} \exp\{-\beta(-(E_1 - E_0) + \mu)\}, \tag{1b}$$

when it is deleted.

Here E_0 is the energy of structure before gas molecule adsorption, E_1 is the energy with gas molecule inserted in a random position, M is the number of gas molecules before the random insertion, V is volume, $\beta = 1/k_BT$, Λ is thermal de Broglie wavelength, and μ is gas chemical potential.

The second step of the doping process is the protonation of PANI, i.e., an acid base reaction of the gas molecule with one of the repeating unit of the polymer chain. In this case, a MC simulation in canonical ensemble may be performed. One protonation event consists of breaking a H-Cl bond and forming a N-H bond with an available nitrogen atom. The acceptance probability of a protonation event of a PANI repeating unit with a neighboring HCl molecule is

$$\min[1, P_{pr}],\ P_{pr} = \exp\{-\beta(E_2 - E_1)\}, \tag{2a}$$

and the acceptance probability of the deprotonation event is

$$\min[1, P_{depr}],\ P_{depr} = \exp\{-\beta(E_1 - E_2)\}, \tag{2b}$$

here E_1 is the energy of structure with HCl molecule inserted and E_2 is the energy after protonation of PANI with this molecule.

Rather than using a scheme involving two MC events and the corresponding moves, we have just mentioned, we propose the following united MC protonation event constituted by a simultaneous HCl molecule insertion and protonation of an available nitrogen site in the polymer. In a similar way, a united MC deprotonation event is constituted by a reverse protonation reaction and a HCl molecule deletion. The energy difference associated with this event equals simply $E_2 - E_0$. We suggest the following acceptance probabilities of the united protonation/deprotonation events:

$$P(M \to M+1) = \min\left[1, \frac{V}{\Lambda^3(M+1)} \exp\{-\beta((E_2 - E_0) - \mu)\}\right], \tag{3a}$$

$$P(M \to M-1) = \min\left[1, \frac{\Lambda^3 M}{V} \exp\{-\beta(-(E_2 - E_0) + \mu)\}\right]. \tag{3b}$$

The probability of acceptance of the united event moves (3a) or (3b) is related to the united event energy difference

$$E_2 - E_0 = \Delta E_{Nononded} + \Delta E_{Bonded}, \tag{4}$$

where $\Delta E_{Nononded}$ is the non-bonded energy change associated with the appearance of a protonated site in the polymer matrix and ΔE_{Bonded} is the difference between total bond energy

before and after a protonation event. According to the proposed scheme $\Delta E_{Bonded} = \Delta E_{Bond}$ where ΔE_{Bond} is the energy difference between H-Cl and N-H covalent bonds. It is straightforward to verify that the acceptance probabilities (3) satisfy the detailed balance requirement. Neglecting thermal fluctuations, ΔE_{Bond} may be considered constant and its value is estimated to be -11 kcal/mol.[15] We can consider ΔE_{Bond} as a parameter characterizing the chemical reaction between the gas and the polymer. Then, once that ΔE_{Bond} is fixed, it is possible to calculate, as in usual GC simulations, several system properties, for example, doping level, as a function of the chemical potential of the gas μ.

The method described above was implemented as a modification of GCMC code of LAMMPS package. The implementation is quite straightforward, one protonation site is chosen randomly among the available ones, corresponding energy differences are calculated and the event can be accepted or rejected according to probabilities of Eq. (3). The UEGC MC method was performed using the following procedure involving a combination of an MD and UEGC MC simulations. In particular, each 100 MD steps in *NVT* ensemble are followed by 10^5 UECG attempts. Altogether we used 5×10^4 MD step and 5×10^6 MC steps for each value of μ. In order to relax the densities, the structures obtained at each value of μ were equilibrated using *NPT* simulations.

B. Force field

The polymer-consistent force field (PCFF) was recently used for simulation of PANI.[10,11,16] The potential energy is given as a sum of bonded and nonbonded terms, $E = E_{bonded} + E_{nonbonded}$,

$$E_{nonbonded} = \sum_{i,j} \frac{q_i q_j}{r_{ij}} + LJ_{9-6}(r_{ij}, \sigma_{ij}, \varepsilon_{ij}), \qquad (5)$$

with the summation over all pairs of nonbonded atoms, where r_{ij} is the distance between atoms, q_i are partial charges and σ_{ij}, ε_{ij} are parameters of *LJ* interaction,

$E_{bonded} = E_{bond} + E_{angle} + E_{dihedral} + E_{out-of-plane} + E_{cross-coupling}$ is the sum of terms describing intramolecular bonded interactions: bonds, angles between bonds, and dihedral angles. The description of PCFF and more details can be found, for example, in Pal's paper.[11] In agreement with the results reported by Ostwal,[10] we found that this FF underestimates both PANI-EB and PANI-ES densities by about 10%. For this reason, we introduced a slight modification of nonbonded parameters of this force field. In particular, the σ and ε values we used were taken from COMPASS FF[17] and from GROMOS96[18] (only for nitrogen). These values are slightly different from PCFF ones, but give densities in better agreement with experiments. More details about the employed parameters and their discussion and validation are reported in the supplementary material.[15]

C. MC and MD simulation details

The hybrid particle-field (PF) method was used to generate initial PANI structure.[19] The method is implemented in OCCAM molecular dynamics code[20] and allows to generate realistic chains conformation. In the PF method the nonbonded term is not infinite if the distance between atoms is zero, allowing chains overlapping and conformation relaxations. It was shown that PF method gives a good reproduction of polymer melt structures,[19] PF molecular dynamics was used also to study other soft matter systems as phospholipids in water.[21] In our simulation we only used the PF method to prepare the initial packing of PANI structure. The PANI structure obtained with PF method contained 8 PANI EB chains, each consisting of 20 PANI EB repeating units (24 carbon atoms in one unit). The PANI molecules were constructed by replication of PANI EB repeating unit shown in Fig. 1. The chains were terminated adding to the first and the last repeating unit hydrogen atoms to the carbon and the nitrogen atoms, respectively.

After energy minimization of thus obtained PANI EB structure the MD simulation in *NVT* ensemble was performed. The structure was first simulated at 1000 K for 0.4 ns and then the temperature was decreased to 300 K at a quenching rate 0.5 K/ps. At this temperature it was further simulated in *NPT* ensemble at a pressure of 1 atm. The simulation time was long enough to relax the PANI density. The density of the obtained PANI EB structure was 1.2 g/cm^3.

We used LAMMPS package for MD simulations reported here. For all the results presented an atom pair distance cutoff was set to 10 Å to compute the Lennard-Jones and the real space term of Coulomb interactions. Particle-particle particle-mesh solver was used to calculate the reciprocal space term of Coulomb interaction[22] and the Nose/Hoover thermostat and barostat were used.[23] The time integration was performed with time step ranging from 0.5 to 1 fs depending on the temperature applied.

MC simulations in grand canonical ensemble have been employed to study the water adsorption in PANI structures at different doping levels. Equilibrium structures were obtained in the following way: each 10^5 MC steps were followed by 100 MD step; altogether 3×10^8 GCMC steps for each doping level were performed. We used the value of water chemical potential $\mu_{H_2O} = -5.4$ kcal/mol.[24] After the structures with water were obtained they were equilibrated in *NVT* ensemble.

In the MC simulation the interaction energy of atom/molecules with structure was calculated. The individual pair interactions cannot be calculated in reciprocal space. The Coulomb term of pair interaction of atom i was calculated as

$$E^{coul}(i) = \sum_{j=1..N, j \neq i} \frac{q_i q_j}{r_{ij}}, \qquad (6)$$

where N is the number of atoms in structure, while the van der Waals term was calculated with a cutoff of 10 Å.

The atom coordinates and trajectories obtained by LAMMPS package were used to calculate the structure factors. The structure factors were calculated by ISAACS scattering code using X-ray scattering atom lengths.[25]

The dielectric constant ε of obtained PANI structures was calculated from the Clausius-Mosotti fluctuation formula

$$(\varepsilon - 1)\left(\frac{2\varepsilon_{RF} + 1}{2\varepsilon_{RF} + \varepsilon}\right) = \frac{\langle M^2 \rangle - \langle M \rangle^2}{3\varepsilon_0 V k_B T}, \qquad (7)$$

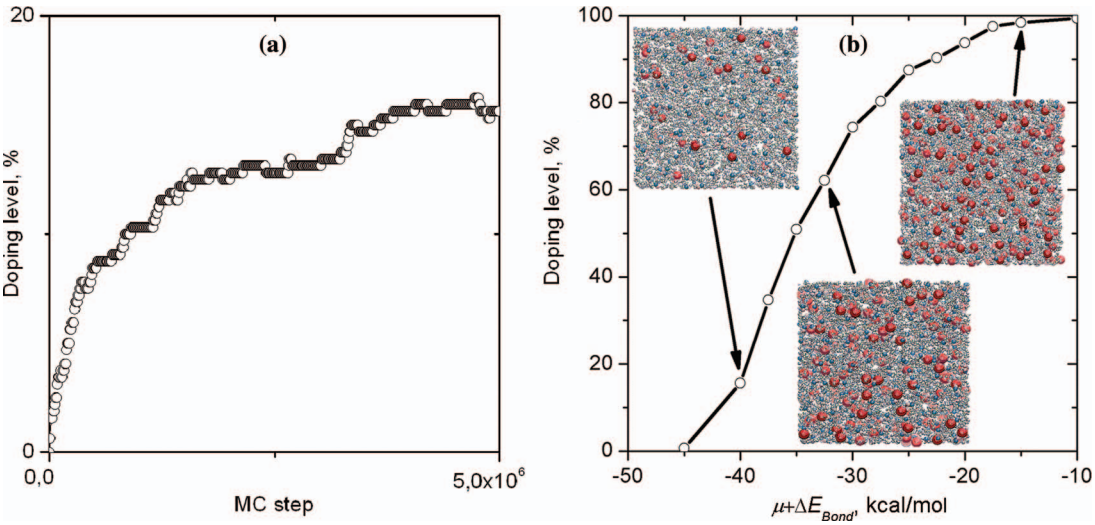

FIG. 2. The MC step dependence (a) and $\mu + \Delta E_{Bond}$ dependence (b) of PANI doping level. The MC step dependence is obtained at $\mu + \Delta E_{Bond} = -40$ kcal/mol. Cl ions are highlighted in red on corresponding structure snapshots.

where M is dipole moment, ε is dielectric constant of vacuum, ε_{RF} is reactive field constant, k_B is the Boltzmann constant, while V and T are volume and temperature.[26]

III. SIMULATION RESULTS

A. Pure PANI

The UEGC procedure described above has been applied to obtain equilibrium PANI structures at different doping levels starting from a relaxed PANI EB structure in which at the beginning no protonated sites were present. As previously explained, once the value of ΔE_{Bond} is fixed structures having different doping levels can be obtained by changing the gas chemical potential μ. When the value of μ is increased, the Boltzmann factor $\exp\{-\beta(E_2 - E_0 - \mu)\}$ of the protonation event (3a) increases and the doping level can start to grow. By running UEGC simulations, we found that the doping level started to increase for values of $\mu + \Delta E_{Bond}$ larger than -45 kcal/mol. The dependence of the doping level on the number of MC steps at $\mu + \Delta E_{Bond} = -40$ kcal/mol is shown in Fig. 2(a). By gradually increasing μ the PANI doping level was gradually increased until pure PANI ES was finally obtained. The $\mu + \Delta E_{Bond}$ dependence of PANI doping level is shown in Fig. 2(b). The obtained structures with different doping levels were further simulated by MD in *NPT* ensemble to relax density. The resulting PANI density is presented in Fig. 3 as a function of doping level. The obtained densities of PANI EB 1.2 g/cm^3 and PANI ES 1.32 g/cm^3 are in good agreement with experimental values 1.24 and 1.33, respectively.[3] The obtained doping level dependence of PANI density is close to linear.

Besides the polymer density, the Hildebrand's solubility parameter is often calculated with the use of atomistic simulation in order to validate the FF and the procedure used. We calculated the Hildebrand's solubility as

$$\delta = \sqrt{\frac{E^{\text{Intermolecular}}}{V}}, \qquad (8)$$

where $E^{\text{Intermolecular}}$ is the energy of interaction between PANI chains. The calculated value of solubility parameter of PANI EB 22.5 MPa$^{1/2}$ is in good agreement with the experimental measurements 22.2 MPa$^{1/2}$.[27] In doped PANI it is not trivial to define intramolecular nonbonded interaction, because Cl ions belong rather to the whole PANI structure than to specific PANI molecule.

Maron *et al.*[28] performed X-ray scattering analyses of amorphous PANI films and reported the experimental structure factors of PANI EB and PANI-HCl. To further validate our model we have calculated the q-weighted structure factors $qS(q)$ of our PANI EB and fully doped PANI–HCl structures and compare them with those obtained by X-ray scattering in Fig. 4. All the peaks of experimental structure factors are reproduced by our model and thus a good agreement with experiment is observed.

In order to analyze the structures coming from the proposed procedure, we considered the radial distribution functions (RDFs) between different atom pairs present in the

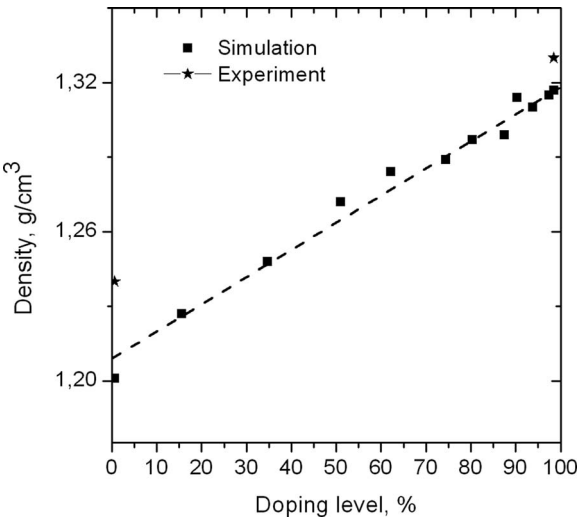

FIG. 3. The doping level dependence of PANI density.

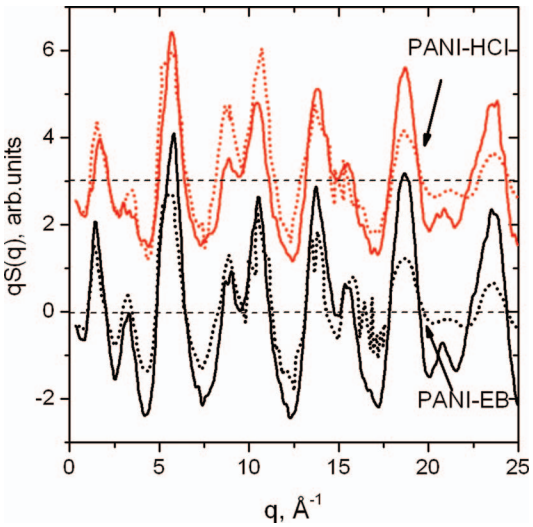

FIG. 4. PANI EB and PANI-HCl structure factors calculated (solid lines) and obtained by X-ray scattering[28] (dotted lines).

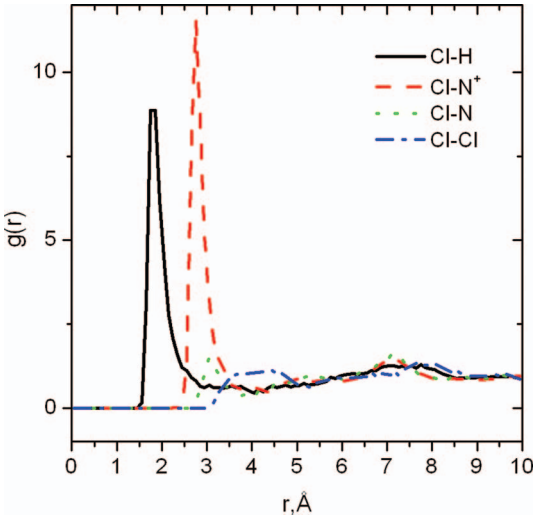

FIG. 5. Pair correlation function in PANI-HCl.

PANI structures. In particular, to analyze the interaction of Cl^- ion with other PANI atoms we have calculated the partial correlation functions for the following pairs Cl-H, Cl-Cl, and Cl-N, where the N ($q < 0$) and doped N^+ ($q > 0$) were considered separately. The RDFs of fully doped PANI are presented in Fig. 5. We obtained stronger correlations between Cl anion and charged nitrogen (N^+) and weaker correlations between Cl with neutral nitrogen atoms (N). A strong interaction of Cl ions with H atoms bonded to both N+ and N was also found. In Fig. 6 we compared the Cl-H and Cl-N+ RDFs for three different values of doping level: 100%, 51%, and 15%. Interestingly, we found that strongest correlations are observed in PANI structures with smaller doping level. The coordination numbers of Cl ion are calculated by counting H or N^+ atom in sphere of radius 3.5 Å and are presented as a function of doping level in insets of corresponding plots. The number of H atoms in neighborhood of Cl ion can be considered as a measure of the correlation between these atoms. The linear decrease of this parameter with doping level is observed on inset of Fig. 6(a). The number of doped N^+ atoms increases with doping level and produces the increase of corresponding coordination number. The smaller correlations at higher doping level may be explained by raise of screening effect on the Coulomb interaction between ions of opposite charges of PANI structures with the increase of Cl ions amount. In order to demonstrate it we have calculated using Clausius-Mosotti equation the values of dielectric constant at different doping levels, and plot the results in Fig. 7. The increase of the dielectric constant with doping level is observed. This increase is consistent with a weaker interaction between charges at high doping levels.

It is shown in inset of Fig. 6(b) that in case of fully doped PANI the number of doped N^+ atoms in the coordination sphere of Cl is 1.6. Some of these N^+ atoms may belong to different PANI chains and thus 1 Cl ion may form hydrogen

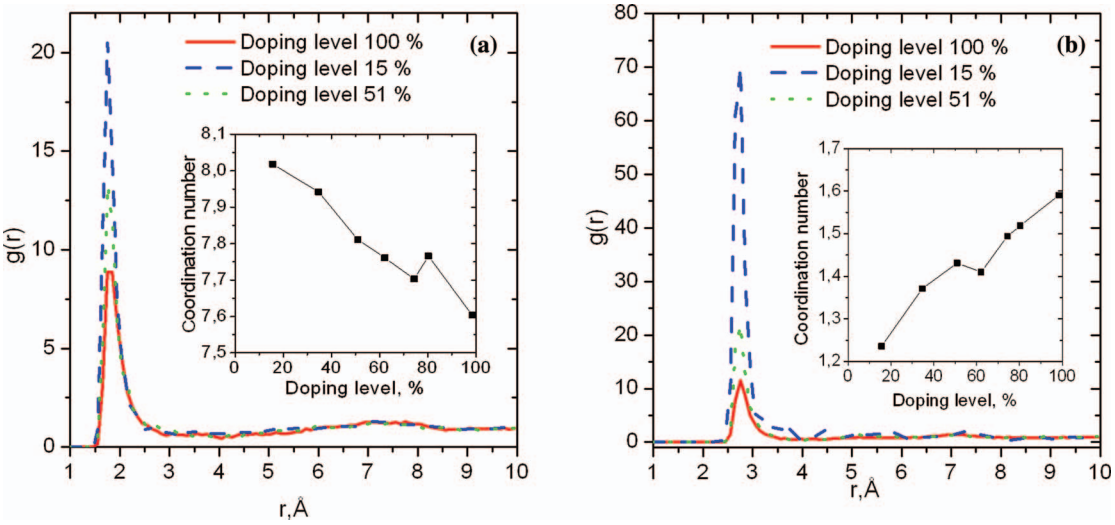

FIG. 6. Cl-H (a) and Cl-N+ (b) pair correlation functions at different doping levels. In insets the corresponding Cl coordination numbers are shown as function of doping level.

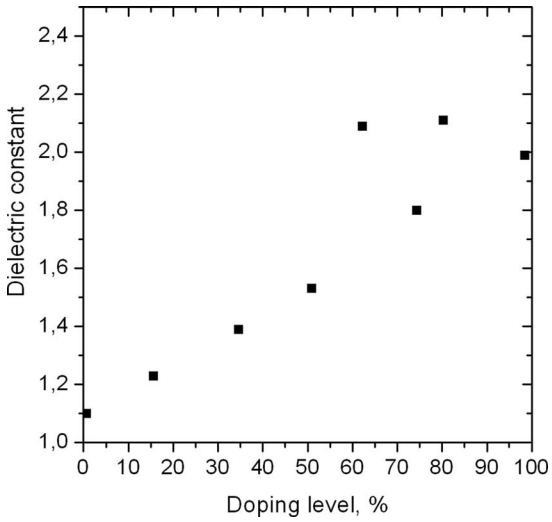

FIG. 7. Doping level dependence of dielectric constant.

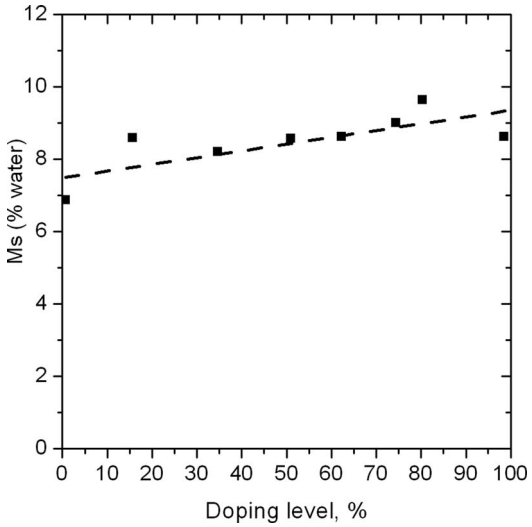

FIG. 8. Doping level dependence of water adsorption.

bonds with more than 1 PANI chain. We calculated the number of chains to which Cl ions are bound. Indeed it turns out that the number of Cl ions forming hydrogen bond with only one chain is close to the number of Cl ions forming bonds with 2 different chains with a non negligible amount of ions forming hydrogen bonds with 3 chains. The distribution of numbers of chains bound to Cl ion is presented in supplementary material.[15] The presence of interchain bridges formed by Cl ions was also reported by Cavazzoni *et al.*[3]

B. Water effect

In order to obtain configurations including water molecules, MC simulation in grand canonical (μTV) ensemble have been performed. The mass fraction of water adsorbed was calculated as

$$Ms(\%) = \frac{M_{Water}}{M_{PANI}} \times 100, \quad (9)$$

where M_{PANI} is the weight of pure PANI, given by mass of all the atoms excluding those of water, and M_{water} is the total weight of all the water molecules adsorbed. It is presented in Fig. 8 as a function of PANI doping level. We have found that doping level dependence of water adsorption is weak. In particular, a slight increase of water adsorption with doping level is observed. The obtained mass fraction of water adsorbed is in the range from 7% to 10%, in reasonable agreement with experimental results. Ostwal *et al.*[29] performed the experimental study of water adsorption by PANI powder. The reported values of content of water adsorbed at relative humidity 80% are 5% for PANI EB and 10% for fully doped PANI-HCl. At the same time they reported a water adsorption of 11% by internally produced PANI EB powder. Canales *et al.*[12] reported that content of water adsorbed by PANI EB may reach 15%.

The pair correlation functions in fully doped PANI with 8.6% water are presented in Fig. 9. In Fig. 9(a) RDF of PANI-HCl with water adsorbed is compared with the ones of pure

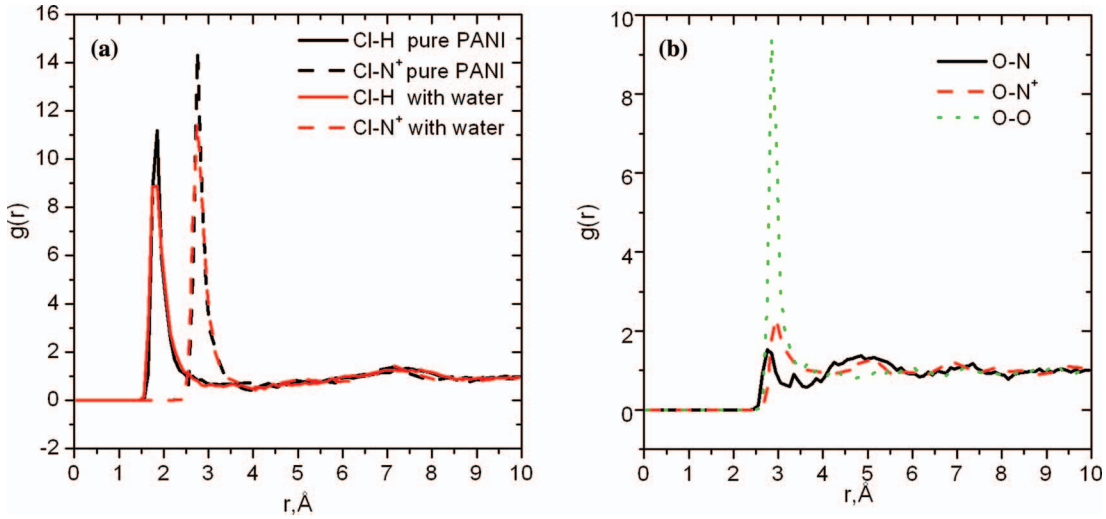

FIG. 9. Pair correlation function in PANI-HCl: (a) Effect of water to Cl-H and Cl-N+ pair correlation and (b) water-water, water-N, and water-N+ pair correlations. Oxygen was considered as the water molecule center.

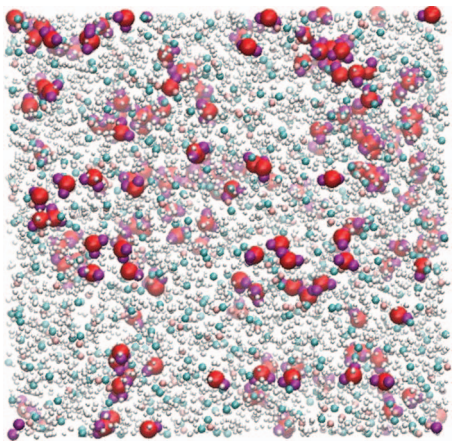

FIG. 10. The snapshot of PANI EB with water adsorbed. Water molecules are highlighted (oxygen atoms in red and hydrogen in purple).

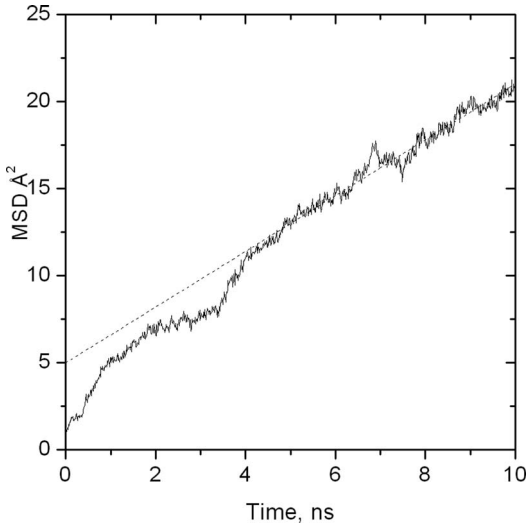

FIG. 11. Time dependence of MSD of water in PANI-HCl.

PANI-HCl. We can see that water affects the correlations between Cl ion and doped N^+ making them slightly weaker. In Fig. 9(b) O-N, O-N+ and O-O pair correlation functions are also presented. The interaction of O atom with both positively charged N^+ and negatively charged N does not produce strong correlations between these atoms. In contrast the sharp peak on the O-O pair correlation function is observed and it indicates self aggregations of water molecules. The self aggregation of water is also observed on the snapshot of structure of PANI with water adsorbed, presented in Fig. 10. The organization of PANI adsorbed water in nanodrops was recently reported by Casanovas *et al.*[30]

The diffusion of water vapor in PANI-HCl was studied by Ostwal.[10] The calculated diffusion coefficient was one order of magnitude higher than that obtained experimentally; this was attributed to low density of their PANI-HCl structures (1.2 g/cm^3). As the density of our PANI-HCl structure (1.32 g/cm^3) is higher than in Ostwal's paper, we expected to obtain a water diffusion coefficient closer to experimental value. The self diffusivity of water vapor in PANI was computed from the mean square displacement (MSD) of water molecules by using $D = \lim_{t\to\infty} \frac{1}{6t} \langle |R(t) - R(0)|^2 \rangle$. The water diffusion depends strongly on amount of water adsorbed. We calculated the MSD of water molecules in PANI-HCl structure with 8.6% water adsorbed. The average MSD of water molecules is presented in Fig. 11 as a function of time, where we see that the linear regime is reached after about 5 ns. The estimated value of the diffusion coefficient is $D = 2.5 \times 10^{-12}$ m^2/s. The obtained value is two times smaller than Ostwal's simulation result, but still higher than the experimental results. The reported values of water diffusion in PANI-HCl are 3×10^{-13} m^2/s in hollow fiber[29] and 4×10^{-14} m^2/s in PANI pellet.[31] The accuracy of the values of diffusion coefficient estimated by MD simulation depends on the PANI density, free volume distribution and on the force field used for PANI-water interaction. As soon as the density of our PANI structure is close to the experimental PANI density, we believe that the PANI-water interaction should be refined to improve agreement with experiments.

In supplementary material[15] we have reported that the united event minimum energy difference $E_2 - E_0$ in freestanding PANI unit calculated using the FF employed in our simulation is about −24 kcal/mol. It was possible to calculate the united event energy differences $E_2 - E_0$ corresponding to all the Cl ions present in equilibrated PANI separately. The distribution of $E_2 - E_0$ in PANI-HCl structures is very instructive and is presented in Fig. 12(a). One can see that the average value of $E_2 - E_0$ in amorphous PANI structure is about twice lower than the value calculated for freestanding PANI unit. This is not surprising for the presence of more interaction sites in a dense bulk structure with the respect to an isolated PANI unit. More interesting is the wide distribution of $E_2 - E_0$ values going from −70 to −30 kcal/mol found for the fully doped amorphous PANI (black curve of Figure 12(a)). Low values $E_2 - E_0$ correspond to sites having strong binding energies, while high values of $E_2 - E_0$ correspond to sites having weaker binding energies. This picture, describing a wide range of binding sites can help with the interpretation of sensing experiments.

One interesting aspect is the role of water molecules. In Fig. 12(a) we also present the distribution of $E_2 - E_0$ calculated for a system having fully doped amorphous PANI with 8.6% water adsorbed. The effect of water in the distribution is twofold, the distribution of $E_2 - E_0$ is shifted by 10 kcal/mol and is less wide. According to this result, the presence of water molecules has the main effect of a stronger binding of HCl to PANI.

In order to understand this effect the calculated $E_2 - E_0$ can be partitioned in two different contributions due to the interaction of *H, Cl*, and *N* with PANI $(E_2 - E_0)_{PANI}$ and water molecules $(E_2 - E_0)_{WATER}$. The sum of these two terms will give $E_2 - E_0$. The distributions of these energies are shown in Fig. 12(b). For comparison the curve of the system without water is also reported. The distribution obtained for $(E_2 - E_0)_{PANI}$ in the structure with water is almost coincident with the distribution of $E_2 - E_0$ calculated for the system without water. The behavior of $(E_2 - E_0)_{WATER}$ distribution is very interesting. In particular, except a small positive tail all the distribution is characterized by negative values up to −30 kcal/mol. This result indicates that the stronger binding

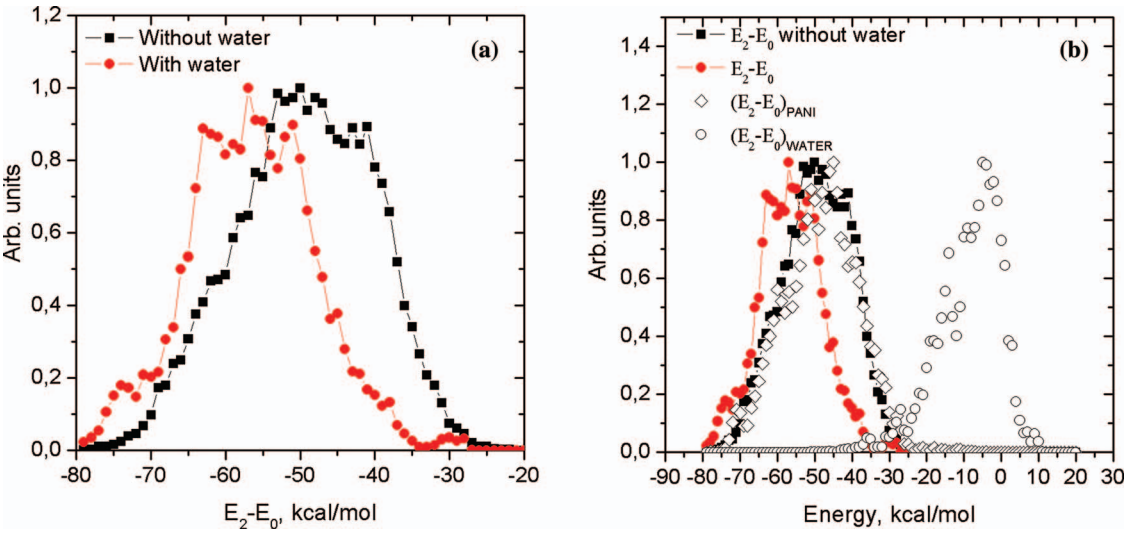

FIG. 12. Distribution of (a) $E_2 - E_0$ in amorphous PANI-HCl with and without water and (b) $E_2 - E_0$ energy partitioned to interaction with PANI and water molecules.

is related mainly to the interactions of *H*, *Cl*, and *N* with water molecules present in the structure.

As discussed above, we expect, in the same conditions, an increase of doping level in the presence of water. This effect can be also studied by atomistic simulation with the use of the proposed UEGC scheme. We compared the behavior of doping level at different values of HCl gas chemical potential μ for pure PANI and for the structure with 8.6% water adsorbed. Differently from previous simulations we started from fully doped structures and decreasing the chemical potential we obtained structures having smaller doping levels up to 0%. As shown in Fig. 13, for the same chemical potential a larger doping level is always obtained for the structure including water molecules. Finally, it is worth noting that the doping level decreases strongly when $\mu + \Delta E_{Bond}$ decreases from -40 to -60 kcal/mol (see Figure 13). This energy interval agrees well with the distribution presented in Fig. 12.

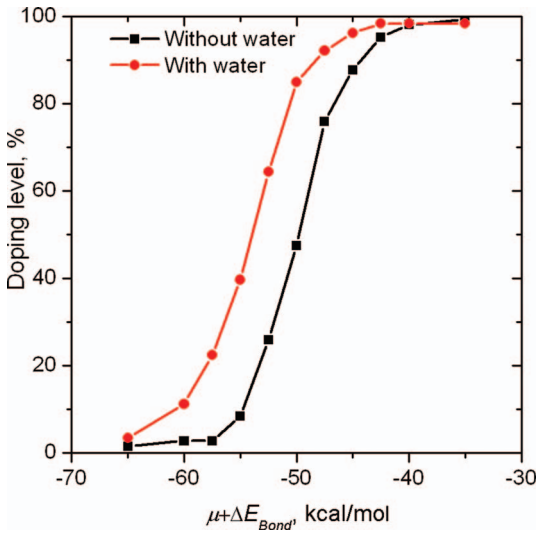

FIG. 13. $\mu+\Delta E_{Bond}$ dependence of PANI doping level at pressure 1 atm in structure of pure PANI and PANI with 8.6% water adsorbed.

Indeed, in the case of pure PANI the distribution of $E_2 - E_0$ is in the range from -35 to -65 kcal/mol and in the presence of water this range is shifted toward lower values by about 10 kcal/mol. This agreement is also an evidence of the good convergence of the method.

IV. CONCLUSIONS

In the present paper a procedure based on a combination of UEGC Monte Carlo and Molecular Dynamics is proposed for the generation of partially doped PANI structures. This procedure is general and the proposed UEGC Monte Carlo scheme can be easily extended to similar polymeric materials used in gas sensing and to other systems involving adsorption and chemical reactions steps. The accuracy of the empirical force field used for the study of PANI is validated also by comparison with DFT calculations and several experimental data. Starting from the configurations obtained with the proposed procedure an atomistic study of amorphous PANI structures at different doping levels has been performed. The density of PANI has been computed as function of doping level. The calculated structure factors, density and solubility parameters values are in good agreement with experimental results.

The adsorption of water by PANI structure has been also studied. The calculated content of adsorbed water, in agreement with experimental studies, is in the range from 8% to 10% for doping level ranging from 0% to 100%. Furthermore, clustering of adsorbed water is observed.

From the pair correlation analysis, it is found that increase of PANI doping level makes these correlations weaker. This behavior has been rationalized by an increase of PANI dielectric constant with doping level.

The picture emerging from the simulations describes a wide range of binding sites having different interaction energies with the reacted HCl molecules in the PANI amorphous structures. It is shown that adsorption of water by PANI makes these interactions stronger and can favor the doping process.

This picture is confirmed by the results of UECG simulations: in all cases for the same chemical potential a larger doping level is always obtained for the structure including water molecules. The PANI electrical conductivity and its response to gas will be studied using partially doped atomistic structures, obtained using the proposed method, in future works.

ACKNOWLEDGMENTS

This study was supported by IMPRESA (Impiego di materiali polimerici composite per la Realizzazione di Sensori integrati in dispositive a basso costo in Applicazioni multisensoriali) Project DM60704 of the MIUR Italy. G.M. thanks MIUR PRIN-2010-2011 (*Meccanismi di attivazione della CO_2 per la progettazione di nuovi materiali per l'efficienza dell'energia e delle risorse*). M.S.B. is grateful to Antonio De Nicola for numerous discussions of simulation details.

[1]A. G. MacDiarmid, Angew. Chem., Int. Ed. **40**(14), 2581 (2001).
[2]T. A. Skotheim and J. Reynolds, *Handbook of Conducting Polymers* (CRC Press, Boca Raton, 2007).
[3]C. Cavazzoni, R. Colle, R. Farchioni, and G. Grosso, Phys. Rev. B **74**(3), 033103 (2006).
[4]A. Varela-Álvarez, J. A. Sordo, and G. E. Scuseria, J. Am. Chem. Soc. **127**(32), 11318 (2005).
[5]J. Stejskal, D. Hlavatá, P. Holler, M. Trchová, J. Prokeš, and I. Sapurina, Polym. Int. **53**(3), 294 (2004).
[6]N. E. Agbor, M. C. Petty, and A. P. Monkman, Sens. Actuators B **28**(3), 173 (1995); M. M. Ayad, N. A. Salahuddin, M. O. Alghaysh, and R. M. Issa, Curr. Appl. Phys. **10**(1), 235 (2010); J. Huang, S. Virji, B. H. Weiller, and R. B. Kaner, Chem. Eur. J. **10**(6), 1314 (2004); J. Janata and M. Josowicz, Nature Mater. **2**(1), 19 (2003).
[7]H. Bai and G. Shi, Sensors **7**(3), 267 (2007).
[8]J. Casanovas, M. Canales, C. A. Ferreira, and C. Alemán, J. Phys. Chem. A **113**(30), 8795 (2009); S.-S. Liu, L.-J. Bian, F. Luan, M.-T. Sun, and X.-X. Liu, Synth. Met. **162**(9–10), 862 (2012); A. Varela-Álvarez and J. A. Sordo, J. Chem. Phys. **128** (17), 174706 (2008).
[9]R. Colle, P. Parruccini, A. Benassi, and C. Cavazzoni, J. Phys. Chem. B **111**(11), 2800 (2007).
[10]M. M. Ostwal, M. Sahimi, and T. T. Tsotsis, Phys. Rev. E **79**(6), 061801 (2009); M. M. Ostwal, T. T. Tsotsis, and M. Sahimi, J. Chem. Phys. **126**(12), 124903 (2007).
[11]S. Pal, G. Balasubramanian, and I. K. Puri, J. Chem. Phys. **136**(4), 044901 (2012).
[12]M. Canales, D. Aradilla, and C. Alemán, J. Polym. Sci. B **49**(18), 1322 (2011).
[13]X. Chen, C. A. Yuan, C. K. Y. Wong, H. Ye, S. Y. Y. Leung, and G. Zhang, Sens. Actuators, B **174**, 210 (2012).
[14]D. Frenkel and B. Smit, *Understanding Molecular Simulation: From Algorithms to Applications* (Academic Press, San Diego, 2002).
[15]See supplementary material at http://dx.doi.org/10.1063/1.4848697 for FF parameter and DFT calculations.
[16]X. P. Chen, C. A. Yuan, C. K. Y. Wong, S. W. Koh, and G. Q. Zhang, Mol. Simul. **37**(12), 990 (2011).
[17]H. Sun, J. Phys. Chem. B **102**(38), 7338 (1998).
[18]C. Oostenbrink, A. Villa, A. E. Mark, and W. F. Van Gunsteren, J. Comput. Chem. **25**(13), 1656 (2004).
[19]G. Milano and T. Kawakatsu, J. Chem. Phys. **130**(21), 214106 (2009).
[20]Y. Zhao, A. De Nicola, T. Kawakatsu, and G. Milano, J. Comput. Chem. **33**(8), 868 (2012).
[21]A. De Nicola, Y. Zhao, T. Kawakatsu, D. Roccatano, and G. Milano, J. Chem. Theory Comput. **7**(9), 2947 (2011); Theor. Chem. Acc. **131**(3), 1 (2012).
[22]R. Hockney and J. Eastwood, *Computer Simulation Using Particles* (Adam Hilger, New York, 1989).
[23]G. J. Martyna, D. J. Tobias, and M. L. Klein, J. Chem. Phys. **101**(5), 4177 (1994); W. Shinoda, M. Shiga, and M. Mikami, Phys. Rev. B **69**(13), 134103 (2004).
[24]J. Hermans, A. Pathiaseril, and A. Anderson, J. Am. Chem. Soc. **110**(18), 5982 (1988).
[25]S. Le Roux and V. Petkov, J. Appl. Cryst. **43**(1), 181 (2010).
[26]R. Clausius, *Die mechanische wärmetheorie* (Vieweg, Braunschweig, 1879); I. G. Tironi and W. F. Van Gunsteren, Mol. Phys. **83**(2), 381 (1994).
[27]R. Jain and R. V. Gregory, Synth. Met. **74**(3), 263 (1995); J. E. Mark, *The Polymer Data Handbook* (Oxford University Press, Incorporated, 2009); L. W. Shacklette and C. C. Han, MRS Online Proc. Lib. **328**, 157 (1993).
[28]J. Maron, M. J. Winokur, and B. R. Mattes, Macromolecules **28**(13), 4475 (1995).
[29]M. M. Ostwal, B. Qi, J. Pellegrino, A. G. Fadeev, I. D. Norris, T. T. Tsotsis, M. Sahimi, and B. R. Mattes, Ind. Eng. Chem. Res. **45**(17), 6021 (2006).
[30]J. Casanovas, M. Canales, G. Fabregat, A. Meneguzzi, and C. Alemán, J. Phys. Chem. B **116**(24), 7342 (2012).
[31]J. P. Travers and M. Nechtschein, Synth. Met. **21**(1–3), 135 (1987).